RSC Advances

PAPER

View Article Online
View Journal | View Issue

Cite this: *RSC Adv.*, 2017, **7**, 24410

A high-safety PVDF/Al_2O_3 composite separator for Li-ion batteries *via* tip-induced electrospinning and dip-coating†

Dezhi Wu,*[a] Lei Deng,[b] Yu Sun,[b] Kwok Siong Teh,[c] Chuan Shi,[d] Qiulin Tan,[e] Jinbao Zhao,[f] Daoheng Sun[a] and Liwei Lin*[ag]

Received 5th March 2017
Accepted 26th April 2017

DOI: 10.1039/c7ra02681a

rsc.li/rsc-advances

Composite membranes have been fabricated made of ultrafine PVDF fibers *via* a tip-induced electrospinning (TIE) process and Al_2O_3 nanoparticles *via* a dip-coating process. These membranes exhibit good thermal stability and electrochemical properties as the separators for applications in lithium ion batteries (LIBs). Experimental results show that the as-fabricated separators may mechanically contract less than 2% when kept at a high temperature of 140 °C for an hour showing good thermal stability as compared with commercial polypropylene separators and electrospun PVDF membranes. The membrane has a measured porosity of 55.8% and ionic conductivity of 2.23 mS cm^{-1}, achieving a low battery discharge capacity loss of 1.8% after 100 cycles in the 1.0C-rate tests, and a retention rate of 92.9% in the 4C-rate tests. These results show the great potential of PVDF/Al_2O_3 separators in LIB applications under high temperature and high current/power operations.

1. Introduction

Lithium-ion batteries (LIBs) are widely used in portable electronics (laptops, intelligent watches, and cell phones) and hybrid/all-electric vehicles.[1,2] As an important component of LIBs, a porous separator facilitates ion transport and prevents electrical contact between the anode and the cathode for safe operations of the battery.[3] Commercial separators based on polyolefin such as polypropylene (PP), polyethylene (PE) and a laminate of PP/PE/PP membrane offer the advantages of low cost, superb mechanical strength, and good chemical stability. However, they have low melting temperatures with general hydrophobic properties and have poor wetting characteristics in liquid electrolytes and thermal shrinkage, leading to low electrolyte uptake, poor conductivity and fracture under harsh conditions such as abnormal heating.[4–6] A gel polymer electrolyte (GPE) membrane is another type of separator and it can be dated back to the 1990s. A variety of polymers and different composite forms of GPE membranes have been developed including PVDF, PAN, PMMA, PVDF–HFP, PAN/Al_2O_3, PVDF/SiO_2 and PVDF–HFP with polyolefin membrane *etc.*[6,7] Particularly, Bellcore (now Telcordia) utilized a liquid extraction and activation method to fabricate GPE membranes basing on PVDF–HFP for industrial applications about twenty years ago, avoiding moisture-free environment requirements, and they have been proved to be beneficial to the safety of lithium-ion batteries.[7] However their relatively lower ionic conductivity about 1 mS cm^{-1} remains a problem. To date, advances in the separator manufacturing call for high porosity, exceptional thermal stability, and good electrochemistry performance for high current/power operations in elevated temperature environments.

Owing to its unique, tortuous microporous structures, diverse material choices and ease of thickness control, the electrospun nonwoven fibers have the potential to be good LIB separator candidates.[8,9] Various groups have demonstrated separator membranes using various polymer materials, such as polyvinylidene fluoride (PVDF),[10] poly(vinylidene fluoride-*co*-hexafluoropropylene) (PVDF–HFP),[11] polyimide (PI),[12] and polyethylene terephthalate (PET)[13] with up to 80% porosity, up to 400% electrolyte uptake, as good as 3 mS cm^{-1} of ionic conductivity, better cycling performances, and high C-rate capacities.[14] Ding *et al.*[15] and Kimura *et al.*[16] have further verified that separators made by composite materials are able to improve the safety of the batter system. Previously reported electrospun membranes are mostly based on a single-spinneret

[a]*Dept. of Mechanical & Electrical Engineering, Xiamen University, Xiamen 361005, China. E-mail: wdz@xmu.edu.cn; Fax: +86 5922185927; Tel: +86 5922185927*
[b]*School of Aerospace Engineering, Xiamen University, Xiamen 361005, China*
[c]*School of Engineering, San Francisco State University, San Francisco 94132, USA*
[d]*Industrial Research Institute of Nonwovens & Technical Textiles, Qingdao University, Qingdao 266071, China*
[e]*Science and Technology on Electronic Test and Measurement Laboratory, North University of China, Taiyuan 030051, China*
[f]*College of Chemistry and Chemical Engineering, Xiamen University, Xiamen 361005, China*
[g]*Department of Mechanical Engineering, University of California at Berkeley, California 94720, USA. E-mail: lwlin@berkeley.edu*

† Electronic supplementary information (ESI) available. See DOI: 10.1039/c7ra02681a

electrospinning. The fiber diameter and pore area distribution of such membranes were well controlled and they performed well as lithium-ion battery separator. However, the actual application of industrialization of the membrane was limited because of the low throughput of single-spinneret electrospinning. Large-scale electrospinning including Dosunmu[17] and Niu·H.[18] have been demonstrated to increase the nanofiber throughput and several commercially available tools have been shown to have industrial-level productions. To this end, in order to apply nanofiber-based membranes for separators in battery systems, it is necessary to study their electrochemical properties.

In this paper, a tip-induced electrospinning (TIE) process is introduced to fabricate PVDF membranes, where multiple tips are mechanically dipped into and removed from the polymer solution to repeatedly generate small liquid spikes on the surface of the polymer solution. With the help of a strong vertical electrical field, liquid jets from the top of these spikes can be initiated and extended to deposit nanofibers on the collector to make nonwoven membranes. Compared with the gel PVDF electrolyte, PVDF membranes prepared by TIE process with high porosity can absorb more liquid electrolyte and get higher lithium-ion conductivity, then improve the performance of lithium battery. The productivity of TIE can reach *ca.* 6 g h^{-1}, the practical application of such membrane can be guaranteed. However, our battery testing results indicate these membranes from the TIE process usually suffer the current leakage problem due to its uneven pore distributions and high porosity. In order to address this problem and improve the thermal stability, Al_2O_3 nanoparticles are incorporated into the membrane to make composite separators using a dip-coating method. Compared to the PE separator and other bare PVDF membranes, the resulting separator has resulted in better thermal stability with shrinkage of about 2% under 140 °C.[3,19] The liquid electrolyte uptake and Li-conductivity of the composite separator decreased after the dip-coating process, but it still showed stable cyclic performance and excellent rate capacities, making it become a promising commercial separator for LIBs.

2. Experimental

2.1 TIE setup and preparation of PVDF separator

PVDF ($M_w \sim 1\,000\,000$, Sensure, Shanghai) was dissolved in a solvent mixture at 16 wt% concentration, which was made up of *N*-methyl-2-pyrrolidone (NMP) & acetone at an equal volume ratio. In order to obtain uniform PVDF fibers, 1 wt% of sodium dodecyl sulfate ($C_{12}H_{25}SO_4Na$, SDS) was added in the PVDF solution. Fig. 1a shows schematic diagram of a TIE setup, which includes a high voltage power supply (GAMMA, USA), thirteen-tip electrode with a tip-to-tip distance of 10 mm, an actuator to mechanically move the electrode into and out of the solution, a solution tank and a grounded collector. PVDF solution was stored in the solution tank and was electrically connected to the anode of the power supply. The collector is grounded and connected to the cathode of the power supply. The experiments were performed for half an hour each time and kept the moving distance of the needles be the same by actuator. The maximum of dipping depth into the solution was kept about 1 mm to maintain jetting of each Taylor cone for a few while, avoiding the reduction of the fiber production efficiency. During the electrospinning process, the change of the dipping depth could be nearly neglected because of the total mass loss was only about twenty grams.

2.2 Preparation of PVDF/Al_2O_3 composite separator

Al_2O_3 (particle size: 400 nm, Taimei Chemicals, Japan) particles and polyethylene oxide (PEO) powder were added into 8 wt% PE solution, where the PEO powder (Changchun Dadi Fine Chemical co., Ltd.) promoted the adhesion between fiber and Al_2O_3 particles, whereas PE (Michelman, China) helped to disperse Al_2O_3 particles. The weight of PEO powder and Al_2O_3 particles were 0.8 wt% and 3.2 wt%, respectively, with respect to the PE solution. The PVDF/Al_2O_3 composite separators were subsequently obtained by dipping PVDF nanofiber membrane into the Al_2O_3 solution for 30 min and removed vertically out of the solution, as shown in Fig. 2.

2.3 Characterization

The morphologies of the electrospun membrane before and after the coating process were characterized by scanning electron microscopy (SEM Su70, Germany) after a thin coating (~10 nm) of gold. Mechanical property was tested on a universal testing machine (UTM4000, SUNS, Shenzhen). The contact angle of the sample was performed on JC2000C1 (Powereach, Shanghai). Thermal shrinkage tests at various temperatures were carried out in an incubator (DHG 9011A, jinghong Shanghai), at 1 hour per specimen to evaluate the dimensional stability of the membranes.

Ionic conductivity and electrochemical properties were also measured by an AC impedance spectroscopy using the electrochemical workstation (AUT84892, Metrohm). The CR2016-type coin cells, Li/separator & electrode/$LiMn_2O_4$ (Qingdao Xinzheng Material Co., Ltd, China) were assembled in a glove box for electrochemical measurements. The electrolyte LB-303 composed of EC/DEC/DMC 1 : 1 : 1 (wt/wt/wt) and 1 mol L^{-1} $LiPF_6$, was purchased (Zhangjiagang Guotai-Huarong New Chemical Materials Co., Ltd, Jiangsu) and used without further purification. A mixture of 90 wt% $LiMn_2O_4$, 5 wt% PVDF, 4 wt% acetylene black, and 1 wt% graphite covered on aluminum foils was used as the positive electrode, and a lithium metal plate was functioned as the counter electrode. A multi-channel battery tester (LAND, China) was utilized to perform the tests of the charge/discharge and cycle stability of the cell.

3. Results and discussions

3.1 TIE process

As seen in Fig. 1b, the multiple-tip electrode can be inserted into and removed from the PVDF solution repeatedly to induce Taylor cones on the surface of the solution due to the viscosity of the polymer solution. As the tips were moving away from the polymer solution, liquid jets were formed on top of the Taylor

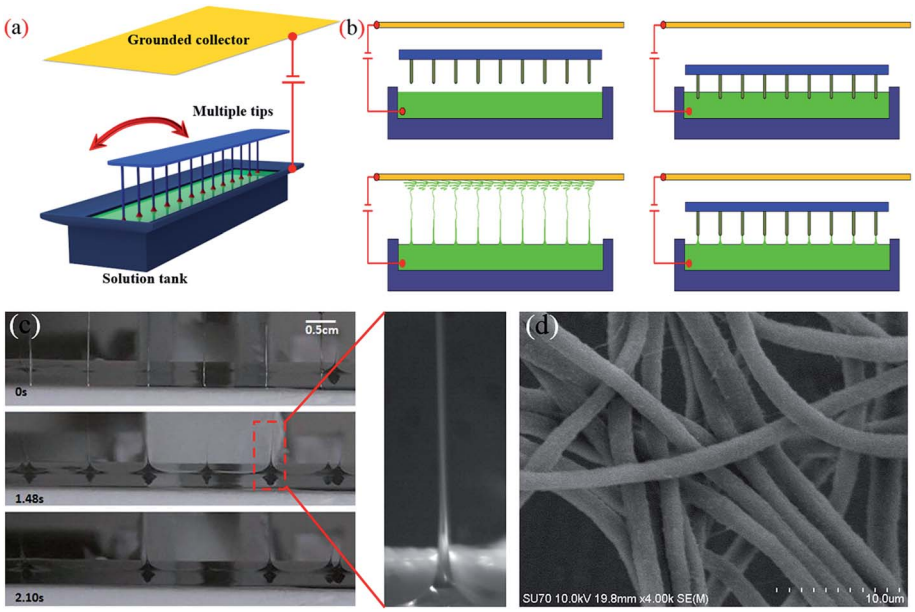

Fig. 1 (a) Schematic diagram of the TIE setup. (b) Illustration of the TIE process. (c) An optical photo showing the generation of Taylor cones and liquid jets at 1.48 and 2.10 seconds of the experiment. (d) A SEM microphoto of ultrafine PVDF fibers deposited on the collector.

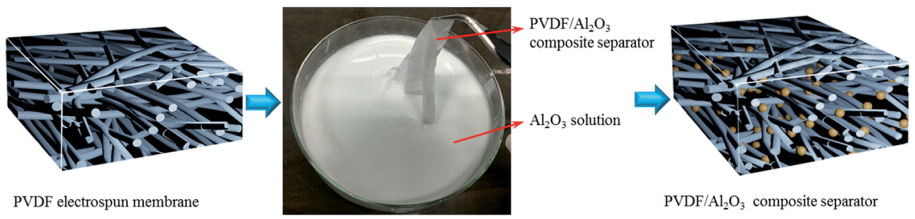

Fig. 2 Preparation of the PVDF/Al_2O_3 composite membrane *via* the dip-coating process.

cones due to the strong electrical field. Fig. 1c shows an optical photo of Taylor cones and liquid jets during the tests. These jets were emitting straight upwards of more than 5 cm to the grounded collector, undergoing bending instabilities, stretching and solvent volatilization before reaching the collector. Fig. 1d shows the SEM photo of the deposited ultrafine fibers.

The effect of applied voltage to the diameter of fibers was investigated in Fig. 3a. As the applied voltage increased from 20 to 45 kV, the mean diameter of the fibers decreased from 3.7 to 2.34 μm due to the higher electrical field. When the applied voltage was 40 kV, the fiber diameter mainly ranged between 1.6 to 4.4 μm with a mean diameter of *ca.* 2.34 μm in Fig. 3b. In this work, the working distance and the applied voltage were set at 40 cm and 40 kV, respectively, to produce PVDF nonwoven membranes with good morphology.

3.2 Morphologies of PVDF and PVDF/Al_2O_3

Fig. 4 shows the average diameter and thickness of the PVDF membranes by the TIE process is about 2.34 μm and 69 μm, respectively, before the nanoparticle coating process. After the dip-coating process and drying for 2 hours at 60 °C, the thickness of PVDF/Al_2O_3 composite separator increased to *ca.* 74 μm, due to the embedment of Al_2O_3 particles. It is found that Al_2O_3 nanoparticles were incorporated and distributed in the PVDF membrane. The nanoparticles seem to attach to the surrounding fiber networks with the assistance of the PEO solutions.

3.3 Porosity, electrolyte uptake and wettability

The porosity (P) of the separator affects the electrolyte uptake and ionic conductivity.[9] The *n*-butanol uptake method is used to evaluate the porosity here as expressed by:[20]

$$P(\%) = M_{\mathrm{BuOH}}/(\rho_{\mathrm{BuOH}} \times (M_{\mathrm{BuOH}}/\rho_{\mathrm{BuOH}} + M_{\mathrm{P}}/\rho_{\mathrm{P}})) \times 100\% \quad (1)$$

where M_{P} and M_{BuOH} represent the masses of membrane before and after the *n*-butanol absorption respectively; ρ_{BuOH} and ρ_{P} represent the densities of the *n*-butanol and polymer, respectively. As shown in Table 1, the porosity of PVDF/Al_2O_3 composite separator was found to be *ca.* 55.8%, which is higher than that of a commercial PP separator at 39.2%. The electrolyte uptake (EU) can be expressed as:

$$\mathrm{EU}(\%) = (W - W_0)/W_0 \times 100\% \quad (2)$$

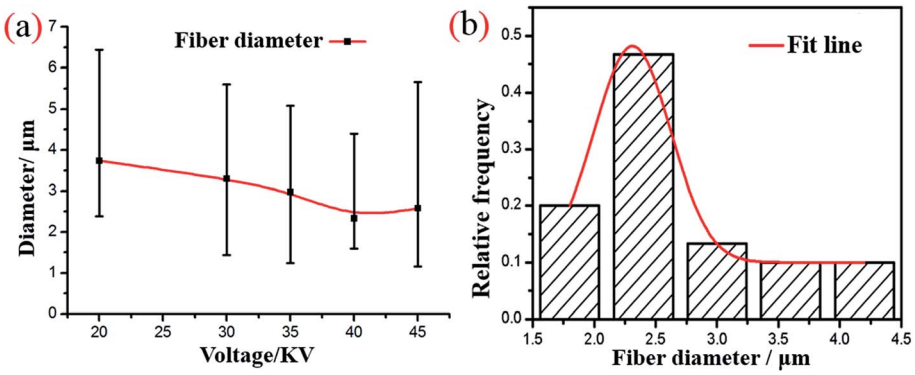

Fig. 3 (a) Experimental characterizations of the fiber diameter *versus* the applied voltage with a fixed liquid solution surface-to-collector distance of 40 cm. (b) Experimental characterizations of the diameter distributions of PVDF fibers under an applied voltage of 40 kV.

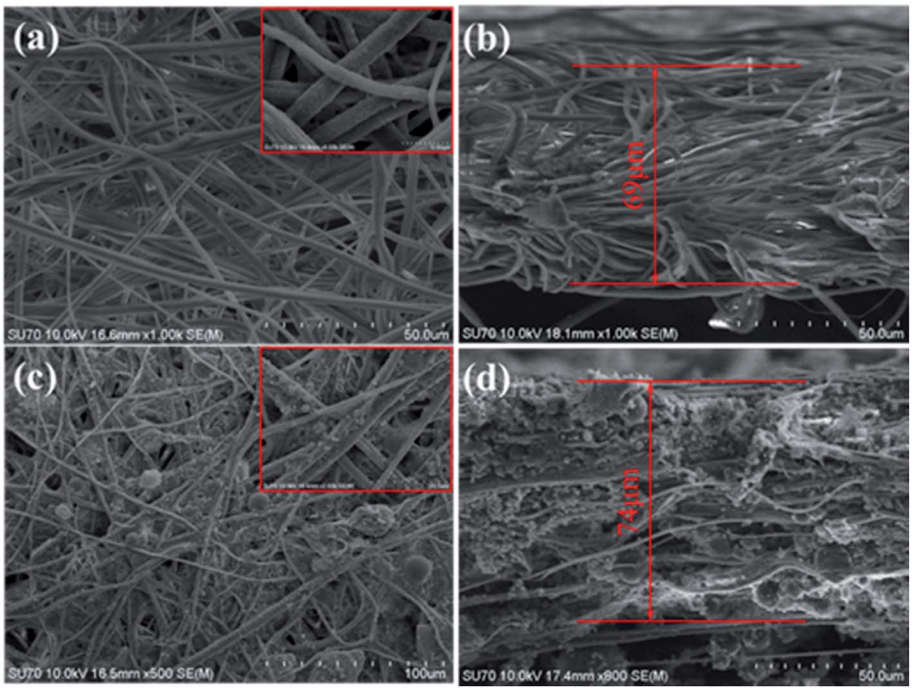

Fig. 4 SEM photos: (a & c) top views of a PVDF membrane and a PVDF/Al_2O_3 composite membrane, respectively. (b & d) Cross-sectional SEM photos showing the morphologies a PVDF membrane and PVDF/Al_2O_3 composite membrane.

where W_0 and W represent the masses of the dry membrane and wet electrolyte-filled membrane, respectively. Separators made by PP, PVDF and PVDF/Al_2O_3 were tested and the average electrolyte uptake for each of these separator materials were 62.9%, 405.1% and 152.4%, respectively. These numbers imply that the porosity and electrolyte uptake of PVDF/Al_2O_3 composite separator are weakened by the incorporation of Al_2O_3 particles but they are still superior as compared with the PP membrane.

Table 1 Porosity and electrolyte uptake of PP, PVDF and PVDF/Al_2O_3 separators

Separator	P (%)	EU (%)
PP	39.2 ± 1.51	62.9 ± 3.34
PVDF	75.0 ± 1.19	405.1 ± 12.51
PVDF/Al_2O_3	55.8 ± 0.48	152.4 ± 4.77

Excellent wettability helps to retain the electrolyte and facilitates the ion diffusion process in the LIB.[3] The contact angle of the separator is used to characterize the separator's wettability in electrolyte. The angle was measured three seconds after a drop of electrolyte was in contact with the separator. Fig. 5 shows that the contact angle of PP is 56° and that of PVDF membrane and PVDF/Al_2O_3 separator are almost zero because the electrolyte has completely saturated the PVDF membrane and PVDF/Al_2O_3 separator. It can be concluded that PVDF and PVDF/Al_2O_3 separators can readily absorb the electrolyte as PVDF has remarkable good affinity to the electrolyte solution. Meanwhile, the high specific surface area of Al_2O_3 particles can

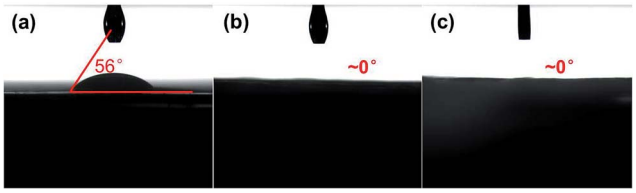

Fig. 5 The measured contact angles of: (a) the PP nonwoven membrane. (b) The PVDF nonwoven membrane. (c) The PVDF/Al_2O_3 composite membrane.

also promote the absorption of electrolyte to accelerate the infiltration of and diffusion of ions in the electrolyte.

3.4 Thermal shrinkage

Many microporous membranes are prone to experiencing shrinkages at elevated temperatures, generating serious safety concerns in LIB applications. Fig. 6 shows that if the temperature was below 100 °C, all three kinds of separators nearly maintained their initial size. The PP separator was seen to be the first one to shrink about 4% at the direction parallel to the machining direction when the temperature rose to 120 °C. With the temperature increased to 140 °C, the electrospun PVDF membrane began to shrink about 4.5% and the commercial PP separator shrank sharply to the extent of fracturing. For comparison, the PVDF/Al_2O_3 composite separator only shrank about 2% at 140 °C and was able to maintain its shape, revealing its excellent thermal resistance due to the support of Al_2O_3 particles.

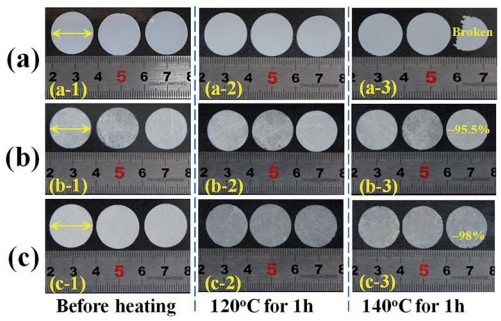

Fig. 6 Photographs of (a) a PP separator. (b) An electrospun PVDF separator and (c) a PVDF/Al_2O_3 composite separator before and after exposures to 120 °C and 140 °C for one hour. The yellow arrow indicates the mechanical stretching direction of the diaphragm and the inserted value represents the thermal shrinkage of the diaphragm.

3.5 Ionic conductivity and battery performance

The ionic conductivity of separator at room temperature was measured by the AC impedance spectroscopy over a frequency range of 1 to 10^5 Hz with an AC amplitude of 5 mV.[21] As shown in Fig. 7a, a sandwiched copper/separator/copper structure was employed. The resistance of the separator saturated with electrolyte can be obtained from the intercept of Z' axis and has been calculated and summarized in Table 2. The average resistances of the PP, PVDF and PVDF/Al_2O_3 composite separators were 1.98 ohm, 0.95 ohm and 1.5 ohm, respectively. Moreover, the ionic conductivity of the PVDF/Al_2O_3 composite separator can be improved to 2.23 mS cm^{-1}, which was in between that of the PP separator (0.79 mS cm^{-1}) and PVDF separator (3.32 mS cm^{-1}). The ionic conductivity of such composite separator was also better than that of polyimide nonwoven separators with polyethylene particles coating.[22]

Additionally, CR2016 LIB coin cells using PVDF/Al_2O_3 composite membranes as the separator were assembled and tested and compared with cells made by the PP and PVDF separators. All cells were measured over 100 cycles at 1.0C. As presented in Fig. 8, the initial capacity of the cells with PP, PVDF, and PVDF/Al_2O_3 separator were 110.5 mA h g^{-1}, 119.1 mA h g^{-1} and 114.2 mA h g^{-1}, respectively. After 100 cycles, retentions capacity of cells containing PP, electrospun PVDF and PVDF/Al_2O_3 composite separator were 93.6%, 96.6% and 98.2%, respectively. The reason for the improvement for the

Table 2 Internal resistance and ionic conductivity of PP, PVDF and PVDF/Al_2O_3 separators

Separator	R_b/ohm	$\overline{R_b}$/ohm	σ/mS cm^{-1}	$\bar{\sigma}$/mS cm^{-1}
PP	1.85	1.98 ± 0.11	0.85	0.79 ± 0.05
	2.11		0.74	
	1.99		0.79	
PVDF	0.82	0.95 ± 0.14	3.61	3.32 ± 0.40
	1.14		2.76	
	0.90		3.59	
PVDF/Al_2O_3	1.23	1.5 ± 0.25	2.44	2.23 ± 0.22
	1.44		2.32	
	1.83		1.93	

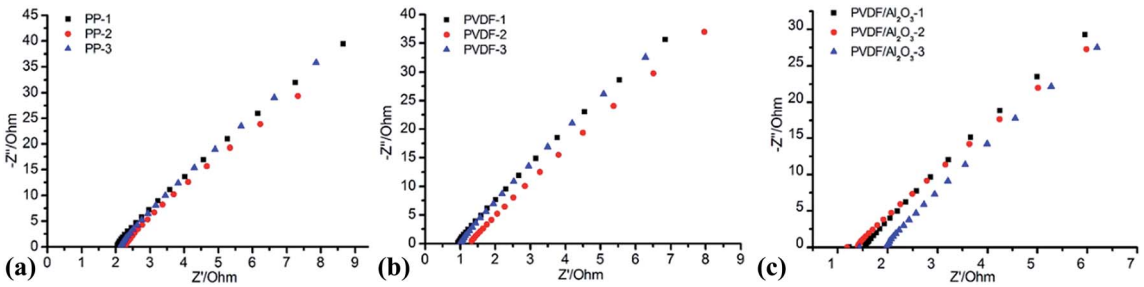

Fig. 7 AC impedance spectroscopies of (a) a PP separator; (b) a PVDF separator and (c) a PVDF/Al_2O_3 composite separator at room temperature.

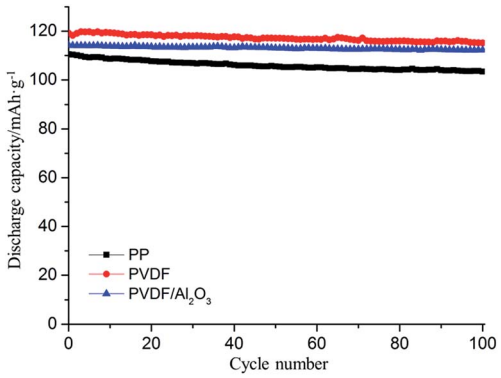

Fig. 8 The discharge capacities of coin cells made by PP, PVDF and PVDF/Al_2O_3 composite separator.

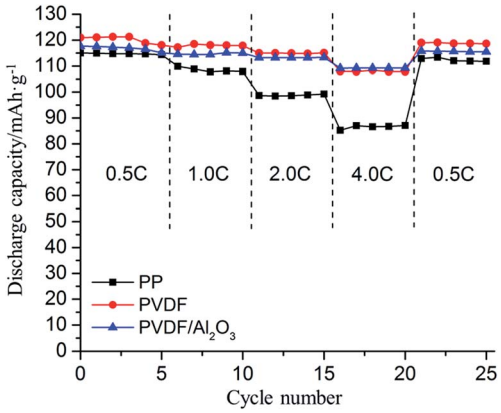

Fig. 9 The rate capacities of cells made by the PP, PVDF and PVDF/Al_2O_3 composite separator.

PVDF/Al_2O_3 composite separator might be that the Al_2O_3 particles can reduce the pore size and alleviate the self-discharge current of the battery. Additionally, the introduction of Al_2O_3 particles can help to prevent the dendrite growth and enhance the battery capacity retention as reported previously.[23]

The rate capacity tests of the Li/$LiMn_2O_4$ cells containing commercial PP, PVDF and PVDF/Al_2O_3 composite separator were carried out by charging the cells at 0.2C to 4.2 V and discharging them at 0.5, 1, 2 and 4C-rate of 5 cycles to 3.6 V in sequence as shown in Fig. 9. When the discharge rate increased from 0.5C to 2C and 4C, the discharge capacity loss for the cell using the PVDF/Al_2O_3 composite separator was 7.1%. Under the same conditions, the cells with the PP separator and PVDF separator were about 24.7% and 11%, respectively. As such, the discharge capacity of LIBs with the composite separator is much better than that with the other two separators for high current/power operation situations. Furthermore, its rate capacity was also better than that (for example, 12.6% discharge capacity loss under 4C discharge rate) of PVDF/PET membranes in our previous work.[24]

4. Conclusion

The manufacturing of composite PVDF/Al_2O_3 separators has been developed by dipping PVDF nanofiber membranes fabricated by the TIE process into the Al_2O_3 suspensions. Their basic properties as potential separator membranes in LIBs have been characterized, including electrolyte uptake, wettability, thermal stability, cycling life, and rate discharge capacity. Results show that the PVDF/Al_2O_3 composite separator has superior thermal stability as compared to the commercial PP separator and the electrospun PVDF membrane separator. Furthermore, the composite separator also possesses a high ionic conductivity of 2.23 mS cm^{-1}, a low discharge capacity decay of 1.8% after 100 cycles under 1.0C-rate discharges, and an excellent retention rate of 92.9% under the 4C-rate discharge operation.

Acknowledgements

This work was supported by the National Science Foundation of China (No. 91648114, U1505243 and No. 51475398) and the Fundamental Research Funds for the Central Universities of China (Xiamen University: No. 20720170037).

References

1 R. Agrawal and G. Pandey, *J. Phys. D: Appl. Phys.*, 2008, **41**, 223001.
2 D. Fu, B. Luan, S. Argue, M. N. Bureau and I. J. Davidson, *J. Power Sources*, 2012, 325–333.
3 S. S. Zhang, *J. Power Sources*, 2007, **164**, 351–364.
4 T.-H. Cho, M. Tanaka, H. Onishi, Y. Kondo, T. Nakamura, H. Yamazaki, S. Tanase and T. Sakai, *J. Electrochem. Soc.*, 2008, **155**, A699–A703.
5 J. Dai, C. Shi, C. Li, X. Shen, L. Peng, D. Wu, D. Sun, P. Zhang and J. Zhao, *Energy Environ. Sci.*, 2016, **9**, 3252–3261.
6 T. Osaka, *Electrochem. Soc. Interface*, 1999, **8**, 9, Batteries Beyond Volta.
7 D.-W. Kim and Y.-K. Sun, *J. Power Sources*, 2001, **102**, 41–45.
8 X. Li, G. Cheruvally, J.-K. Kim, J.-W. Choi, J.-H. Ahn, K.-W. Kim and H.-J. Ahn, *J. Power Sources*, 2007, **167**, 491–498.
9 S. W. Choi, S. M. Jo, W. S. Lee and Y. R. Kim, *Adv. Mater.*, 2003, **15**, 2027–2032.
10 C. Lu, W. Qi, L. Li, J. Xu, P. Chen, R. Xu, L. Han and Q. Yu, *J. Appl. Electrochem.*, 2013, **43**, 711–720.
11 Y. Ding, P. Zhang, Z. Long, Y. Jiang, F. Xu and W. Di, *J. Membr. Sci.*, 2009, **329**, 56–59.
12 Y.-E. Miao, G.-N. Zhu, H. Hou, Y.-Y. Xia and T. Liu, *J. Power Sources*, 2013, **226**, 82–86.
13 J. Hao, G. Lei, Z. Li, L. Wu, Q. Xiao and L. Wang, *J. Membr. Sci.*, 2013, **428**, 11–16.
14 P. Carol, P. Ramakrishnan, B. John and G. Cheruvally, *J. Power Sources*, 2011, **196**, 10156–10162.
15 Y. Ding, P. Zhang, Z. Long, Y. Jiang, F. Xu and W. Di, *J. Membr. Sci.*, 2009, **329**, 56–59.
16 N. Kimura, T. Sakumoto, Y. Mori, K. Wei, B. S. Kim, K. H. Song and I. S. Kim, *Compos. Sci. Technol.*, 2014, **92**, 120–125.
17 O. O. Dosunmu, G. G. Chase, W. Kataphinan and D. H. Reneker, *Nanotechnology*, 2006, **17**, 1123–1127.

18 H. Niu, X. Wang and T. Lin, *Needleless Electrospinning: Developments and Performances*, 2011.
19 J.-A. Choi, S. H. Kim and D.-W. Kim, *J. Power Sources*, 2010, **195**, 6192–6196.
20 J. Kim, S. Choi, S. Jo, W. Lee and B. Kim, *J. Electrochem. Soc.*, 2005, **152**, A295–A300.
21 Y. Zhai, K. Xiao, J. Yu and B. Ding, *Electrochim. Acta*, 2015, **154**, 219–226.
22 C. Shi, P. Zhang, S. Huang, X. He, P. Yang, D. Wu, D. Sun and J. Zhao, *J. Power Sources*, 2015, **298**, 158–165.
23 Q. Liu, M. Xia, J. Chen, Y. Tao, Y. Wang, K. Liu, M. Li, W. Wang and D. Wang, *Electrochim. Acta*, 2015, **176**, 949–955.
24 D. Wu, S. Huang, Z. Xu, Z. Xiao, C. Shi, J. Zhao, R. Zhu, D. Sun and L. Lin, *J. Phys. D: Appl. Phys.*, 2015, **48**, 285305.